Vol. 72: 53–72, 2017
https://doi.org/10.3354/cr01450

CLIMATE RESEARCH
Clim Res

Published online April 5

The impact of climate change on the characteristics of the frost-free season over the contiguous USA as projected by the NARCCAP model ensembles

Shiyuan Zhong[1,*], Lejiang Yu[1], Julie A. Winkler[1], Ying Tang[1], Warren E. Heilman[2], Xindi Bian[2]

[1]Department of Geography, Michigan State University, East Lansing, MI 48824, USA
[2]US Forest Service, Northern Research Station, Lansing, MI 48910, USA

ABSTRACT: Understanding the impacts of climate change on frost-free seasons is key to designing effective adaptation strategies for ecosystem management and agricultural production. This study examines the potential changes in the frost-free season length between historical (1971–2000) and future (2041–2070) periods over the contiguous USA with a focus on spatial variability and the uncertainties surrounding the projections, using daily minimum temperature outputs from a 6-member ensemble composed of 3 regional-climate models nested within 3 general-circulation models provided by the North American Regional Climate Change Assessment Program (NARCCAP). Despite broad agreement among ensemble members on future advance (delay) of last spring (first autumn) frost and thus an increase in the frost-free season length across the USA, large inter-model spread, an indication of high uncertainties, exists especially over the mountainous West. The uncertainty surrounding the first autumn frost is the major contributor to the high uncertainty in the projected frost-free season length for the West, in contrast to other regions, especially the Great Plains, where the ensemble spread in the last spring frost contributes more to the season-length uncertainty. The lengthening is not symmetric in spring and autumn, and the asymmetry, which varies by region and model, is relatively small in the eastern and central USA, and large in the western USA. Across California and portions of the Southwest, the advance in the last spring frost will be more than the delay in the first autumn frost. Elsewhere in the western USA, especially over high terrain, the frost-free season will lengthen more in autumn than in spring.

KEY WORDS: Frost-free season · Frost dates · Growing season · Climate change impact · NARCCAP · Ensemble projection

1. INTRODUCTION

The frost-free season, defined as the period between the last spring frost and the first autumn frost, has a large influence on plant phenology, with implications for the distribution of natural vegetation and the types of crops grown in a particular region (Menzel 2003, Vitasse et al. 2014). Changes in the length of the frost-free season may alter not only agricultural practices and productivity, but also the function and structure of regional ecosystems (United States Environmental Protection Agency [USEPA] 2014).

A number of studies have indicated that the frost-free season in the contiguous USA (CONUS) has experienced substantial changes over the 20th century. For example, Cooter & LeDuc (1995) revealed a significant increasing trend in the length of the frost-free season in the northeastern USA for the period of

*Corresponding author: zhongs@msu.edu

1961–1990. An increasing trend was also observed in the Napa/Sonoma region of California during 1951–1997 (Nemani et al. 2001), and for 6 watersheds in the Catskill Mountains of New York State during 1960–2008 (Anandhi et al. 2013). In addition, a series of technical reports prepared for the latest US National Climate Assessment identified statistically significant upward linear trends in the frost-free season length for the Northeast (Kunkel et al. 2013a), Midwest (Kunkel et al. 2013b), Great Plains (Kunkel et al. 2013c), Southwest (Kunkel et al. 2013d), and Northwest (Kunkel et al. 2013e) regions of CONUS for the period 1895–2011. The average trend was insignificant only in the Southeast region (Kunkel et al. 2013f).

Besides these regional studies, Easterling et al. (2000) and Easterling (2002) reported a significant lengthening of the frost-free season over the second half of the last century across most of CONUS except for the southeastern USA where, similar to the finding of Kunkel et al. (2013f), no statistically significant trend was detected. Moreover, Kunkel et al. (2004) found a 2 wk increase in the nationwide average length of the frost-free season from the beginning to the end of the 20th century. In both studies, the increase in season length was larger for the western USA compared to eastern USA. In a later analysis, Kunkel et al. (2013g) estimated that from 1895 to 2011, the frost-free season west of the 100° W meridian increased, on average, by almost 3 wk; east of 100° W, the average increase was about 10 d. McCabe et al. (2015), focusing on the period from 1920 to 2012, found that although the overall trend in the frost-free season length for CONUS was positive, the magnitude and sign of the trend varied spatially, even between locations in relatively close proximity. Of the 523 stations from the Global Historical Climate Network included in their analysis, approximately half (42 %) had statistically significant positive trends. Significant negative trends were found at 5 % of the stations, most of which were located in the 'warming hole' of the southeastern and south-central USA (e.g. Pan et al. 2004, Meehl et al. 2012). Trends were insignificant at the remaining stations.

Asymmetry in the lengthening of the frost-free season during the 20th and early 21st centuries across CONUS has garnered considerable attention. A number of studies, such as those by Nemani et al. (2001) for coastal California and Kunkel et al. (2013d) for the southwestern USA, attributed the greater season length primarily to an earlier date of last spring frost rather than a delayed date of first autumn frost. Furthermore, the nationwide trends calculated by Kunkel et al. (2004) for the 20th century suggest that for CONUS as a whole, changes in the date of last spring frost have had a larger influence on the lengthening of the frost-free season than changes in the date of first autumn frost. Regional differences are evident, however. Easterling (2002), using regional averages for the period 1948–1999, concluded that the advance in the date of last spring frost was larger than the delay in first autumn frost across most of CONUS, except for the south-central states where the rates of change were similar, and for the southeastern and mid-Atlantic states where the delay in first autumn frost was greater than the advance of last spring frost. On the other hand, Anandhi et al. (2013) found that in the Catskill Mountains of New York, the rate of advance of last spring frost (–2.6 to –4.3 d per decade, depending on watershed) was similar to the delay in first autumn frost (2.7 to 3.2 d per decade). McCabe et al. (2015) argue that whether the lengthening of the frost-free period is asymmetric or symmetric depends on the time period over which the trend is calculated. They found that for CONUS, the beginning of a shift to an earlier date of last spring frost occurred approximately a decade earlier (starting around 1983) than a more recent shift (starting around 1993) to a later date of first autumn frost. Hence, it appears that the lengthening of the frost-free season in the CONUS has become more symmetrical with time in the last 3 decades.

Numerous analyses have suggested that the climate in the 21st century will be significantly different from the historical climate across North America (e.g. Peacock 2012, Collins et al. 2013, Maloney et al. 2014, Romero-Lankao et al. 2014). A question then is whether the increasing trend in the length of the frost-free season in the past will continue into the mid-21st century and beyond. Tebaldi et al. (2006) found an increase in growing-season length in the Northern Hemisphere during the 21st century, based on results from coarse global Atmosphere-Ocean General Circulation Models (AOGCMs) with a horizontal (latitude × longitude) resolution varying from 5° × 4° to 1.125° × 1.125°. Hayhoe et al. (2007), based on ensemble averages of AOGCMs, projected that the growing season in the northeastern USA will be 2 to 4 wk longer by the mid-21st century than during the 1961–1990 period. Similarly, the frost-free season length in the Catskill Mountain region of New York is estimated to increase by 10 to 25 d by 2045–2065 and 13 to 40 d by 2081–2100, depending on the greenhouse gas emissions scenario (Anandhi et al. 2013). Furthermore, Thibeault & Seth (2014) estimated that the length of the frost-free season over the northeastern USA would increase by 12 and 21% by the mid and late 21st century, respectively. Their analysis was based on a larger, 23-member model suite from the Coupled Model Intercomparison Project Phase 5 (CMIP5), whereas both Hayhoe et al. (2007) and Anandhi et al. (2013) employed AOGCM simulations from an earlier phase of CMIP (CMIP3). Using a precipitation-runoff modeling system (PRMS) and simulations from 5 AOGCMs driven by 3 greenhouse gas emissions scenarios (Special Report on Emissions Scenarios [SRES] A1B, B1 and A2), Christiansen et al. (2011) noted an increase by the end of the 21st century of 27 to 47 d in the frost-free season length for 14 river basins across CONUS, with larger increases in the mountainous regions of the western USA. The analysis of simulations from 15 AOGCMs from CMIP5 by Maloney et al. (2014) also suggests that the largest increases by the end of the 21st century in the frost-free season will occur over the western USA.

The coarse resolution of AOGCM simulations has led a number of researchers to infer future changes in frost-free season length from projections that have been dynamically downscaled using regional climate models (RCMs) nested within AOGCMs. In particular, the suite of RCM simulations from the North American Regional Climate Change Assessment Program (NARCCAP, Mearns et al. 2007, 2009) with a 50 × 50 km horizontal resolution was used in the previously mentioned technical reports prepared for the US National Climate Assessment to project mid-century (2041–2070) changes in frost-free season length. Multi-model means from the NARCCAP simulations suggest that under the SRES A2 greenhouse gas emissions scenario, the largest changes (>35 d) in frost-free season length will occur along the US west coast and the high elevations of the Rocky Mountains, with the smallest changes (15 to 20 d) expected in the northern Plains and southern Florida (Kunkel et al. 2013g). For all grid points, >50% of the NARCCAP models indicated a statistically significant change in the frost-free season length, and at least 60% of the members of the NARCCAP model suite agreed on the positive sign of the projected change. In addition, Mote et al. (2013) used the NARCCAP simulation suite to investigate potential increases in frost-free season length for the northwestern USA and found that the multi-model mean changes were larger than the multi-model standard deviations, which could be interpreted as showing that the projected changes are larger than the natural variability. Another regional application of the NARCCAP model suite is provided by Pryor et al. (2013), who estimated that in the midwestern USA, the growing-season length, defined in terms of a cardinal temperature of 4°C, would increase by a factor of 1.16 when averaged across the region and the different ensemble members. Similarly, Patricola & Cook (2013), using a large multi-model ensemble that included the NARCCAP simulations, estimated that the length of the growing season in the Great Plains and the Midwest would increase by 1 to 3 wk by the mid-21st century.

The aforementioned studies have delivered a consistent message that most regions of CONUS will likely experience a longer frost-free season in the future. These projected changes are anticipated to impact natural and human systems, including regional ecosystems and agriculture, and need to be incorporated into environmental and agricultural planning, management, and decision making. However, for these planning activities and decisions to be 'robust', Wilby & Dessai (2010) argue that strategies that perform well across a range of possible future climate conditions are preferable to those that are optimal for 1 climate scenario but may perform badly under a different (but also probable) scenario. Salzmann & Mearns (2012) also argue that the uncertainties of a specific variable generated by climate models need to be evaluated before the model projections can be effectively used by the stakeholder community. Taking this argument farther, Weaver et al. (2013) contend that, for robust decision-making, climate scientists need to provide decision makers with an ensemble of future projections of decision-relevant variables that can be used to obtain insights into complex system behavior and for critical thinking. Consequently, multi-model means of climate projections, which have been the focus of most previous analyses of future frost-free season length, may be insufficient for many planning and decision-making activities, as they did not explicitly discuss the uncertainty surrounding the projected values (Weaver et al. 2013). For this reason, we revisit the NARCCAP simulations that have been used in several earlier studies, but particularly in the US National Climate Assessment technical reports, to consider in more detail the between-model differences in the projected characteristics of the frost-free season that have potential utility to stakeholders. We focus on the NARCCAP simulations rather than the global simulations in the CMIP5 archives, as the spatial resolution of the dynamically downscaled NARCCAP simulations is closer to that often needed for local and regional climate impact, adaptation, and vulnerability assessments (Mearns et al. 2015).

In addition to addressing the uncertainty of the future projections, we provide an assessment of how

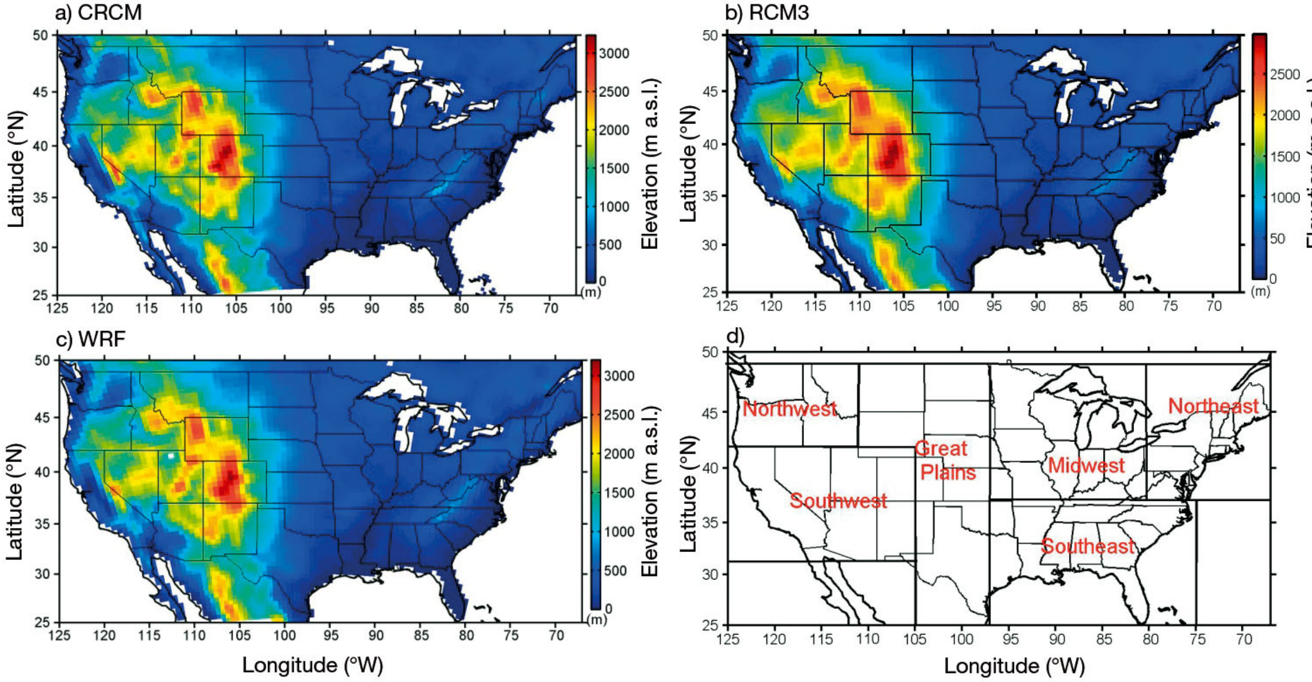

Fig. 1. The domain of the study (25° to 50° N, 67° to 125° W) overlain by the topography (color shading; a.s.l.: above mean sea level) used in the (a) CRCM, (b) RCM3, and (c) WRFG models, and (d) the 6 regions used for the statistical analysis

well the RCMs included in the NARCCAP suite simulate the characteristics of the frost-free season by comparing the model-simulated characteristics for a historical climate period to the characteristics calculated from a gridded reanalysis dataset. This assessment helps to identify the strengths and weaknesses of the different RCMs and contributes to a more informed interpretation of the future projections. A third contribution of our analysis is an evaluation of the (a)symmetry of the projected lengthening of the frost-free season as projected by the NARCCAP simulations. Although, as noted above, several earlier studies analyzed historical trends in the relative changes in the dates of last spring frost and first autumn frost, potential future trends in the symmetry/asymmetry of the lengthening of the frost-free season have not, to our knowledge, been investigated. The nature of the lengthening of the frost-free season has substantial implications for natural vegetation and agriculture. For example, damaging springtime temperatures are currently the major climate-related hazard for the production of many perennial crops (e.g. apple, peach, cherry) in midlatitude growing areas (Winkler et al. 2013a), and production may benefit from an earlier date of last spring frost as long as the crop is not at a more sensitive growth stage (Winkler et al. 2013b). On the other hand, the production of some other perennial crops (e.g. wine grapes) is also limited by lack of maturation at the time of first autumn frost (Jones 2005) and would benefit from a longer delay in its timing.

In sum, the specific objectives of this research are to (1) assess the ability of the NARCCAP model suite to simulate the historical characteristics of the frost-free season, (2) evaluate the level of agreement between the different members of the NARCCAP model suite in terms of the projected future characteristics of the frost-free season for the mid-21st century, with a particular focus on the similarities and differences in the spatial patterns of the projected changes and on the spatial variations in the uncertainty range, and (3) consider changes in the symmetry/asymmetry of the lengthening of the frost-free season by the mid-21st century. The overall intent of these analyses is to provide additional insights regarding future changes in the frost-free season in CONUS for use in environmental and agricultural planning and decision-making.

2. DATA AND METHODS

The domain of this study encompasses CONUS, spanning 25° to 50° N and 67° to 125° W (Fig. 1). The climatology of the frost-free season is characterized by 3 indicators, namely the date of the last spring frost, the date of first autumn frost, and the length of the frost-free season. The dates of last spring frost and first autumn frost are determined using the inclusive threshold of 0°C for daily minimum temperature, and the number of days between the 2 dates defines the length of the frost-free season. Following Easterling (2002), frost occurring prior to 1 July is considered a spring frost event and that occurring on or after 1 July is considered an autumn frost event. Furthermore, if no frost occurs on any day of the year, the frost-free season length is 365 d with 1 January assigned as the date of the last spring frost and 31 December assigned as the date of the first autumn frost (February 29 is ignored).

The daily minimum temperatures over the study domain were obtained from RCM simulations produced by NARCCAP (Mearns et al. 2009). Aimed at generating climate change scenarios for use in regional impact research for North America, NARCCAP produced a set of RCM simulations at 50 km resolution driven by a set of coarse resolution (200 to 300 km) AOGCMs (hereafter referred to as RCM-AOGCMs) for both the historical (1971–2000) climate and the mid-century (2041–2070) climate. The mid-century climate projections were forced by the SRES A2 scenario for the 21st century, which assumes a very heterogeneous world with continuously increasing global population and regionally oriented economic growth (Naki enovi et al. 2000). For the historical climate, NARCCAP also produced another set of RCM simulations for the 1980–2004 period, but instead of AOGCM data, the global reanalysis data produced by the National Centers for Environmental Predictions (NCEP) and the US Department Energy (DOE) (Kalnay et al. 1996, Kanamitsu et al. 2002) were used to force the RCM simulations at the lateral boundaries of their regional domains. Because the NCEP global reanalysis dataset was generated through assimilation of a large set of meteorological observations over the globe into forecast models, a NARCCAP RCM simulation driven by NCEP data at the lateral boundaries (hereafter referred to as RCM-NCEP) has been called the 'perfect boundary condition' simulation (although the NCEP data are not a perfect representation of the atmosphere), in contrast to when a RCM is driven by an AOGCM simulation for a recent climate period. The latter RCM simulation is often referred to as the 'control', 'baseline', or 'reference' simulation, as it is used as a baseline or reference for comparisons with future climate simulations by the same RCM-AOGCM combination (Giorgi 2006, Winkler et al. 2011). The RCM-AOGCM simulations contain not only uncertainties associated with RCMs, but also those inherited from the driving AOGCMs through lateral boundary forcing. Uncertainties in the RCM-NCEP simulations arise mostly from uncertainties in the RCMs.

For the current study, we analyze the daily minimum temperature outputs from 6 combinations between 3 RCMs (CRCM, RCM3 and WRFG) and 3 AOGCMs (CCSM, CGCM3, and GFDL) for the baseline and future climate periods. A description of the NARCCAP models is given in Table S1 (in the Supplement at www.int-res.com/articles/suppl/c072p053_supp.pdf), and their combinations are given in Table S2. The topography used by the 3 RCMs is shown in Fig. 1. We elected not to include the 2 members of the NARCCAP suite involving the HRM3 regional model in this analysis, as earlier comparisons of the HRM3 reanalysis-driven simulations with observations indicated that this RCM performed poorer than the other models, possibly because it is the only model included in NARCCAP suite that was not initially developed for North America (Mearns et al. 2012). In addition to the simulations for the baseline and future climate periods, we analyze the RCM-NCEP simulations for the historical period and compare the results from these 'perfect boundary condition' simulations with those of the RCM-AOGCM baseline simulations to help assess the uncertainties associated with AOGCMs that are introduced from the lateral boundaries into the RCM simulations. The results of the perfect boundary condition and baseline simulations are also compared to the frost-free season characteristics derived from the North American Land Data Assimilation System phase 2 (NLADS-2) gridded reanalysis dataset. NLADS-2 is a quality-controlled, spatially and temporally consistent land-surface dataset from available observations and model output on a 1/8 degree grid over central North America from January 1979 to the present (Cosgrove et al. 2003, Luo et al. 2003). We will simply refer to the results from NLDAS-2 as observations although they are a combination of observations and model outputs, and, as a gridded dataset, NLDAS-2 has limited ability to capture the full spread of the observed values, especially when frosts are in the tails of the local temperature distribution.

The length of the frost-free period is a function of the complex interactions of latitude, topography (e.g. cold air drainage), surface conditions (e.g. snow cover), and the synoptic and sub-synoptic circulation features contributing to radiative and advective freezes, all of which vary spatially. Consequently, we are particularly interested in how the simulated spatial patterns of the frost-free season differ among the NARCCAP simulations for the baseline and future

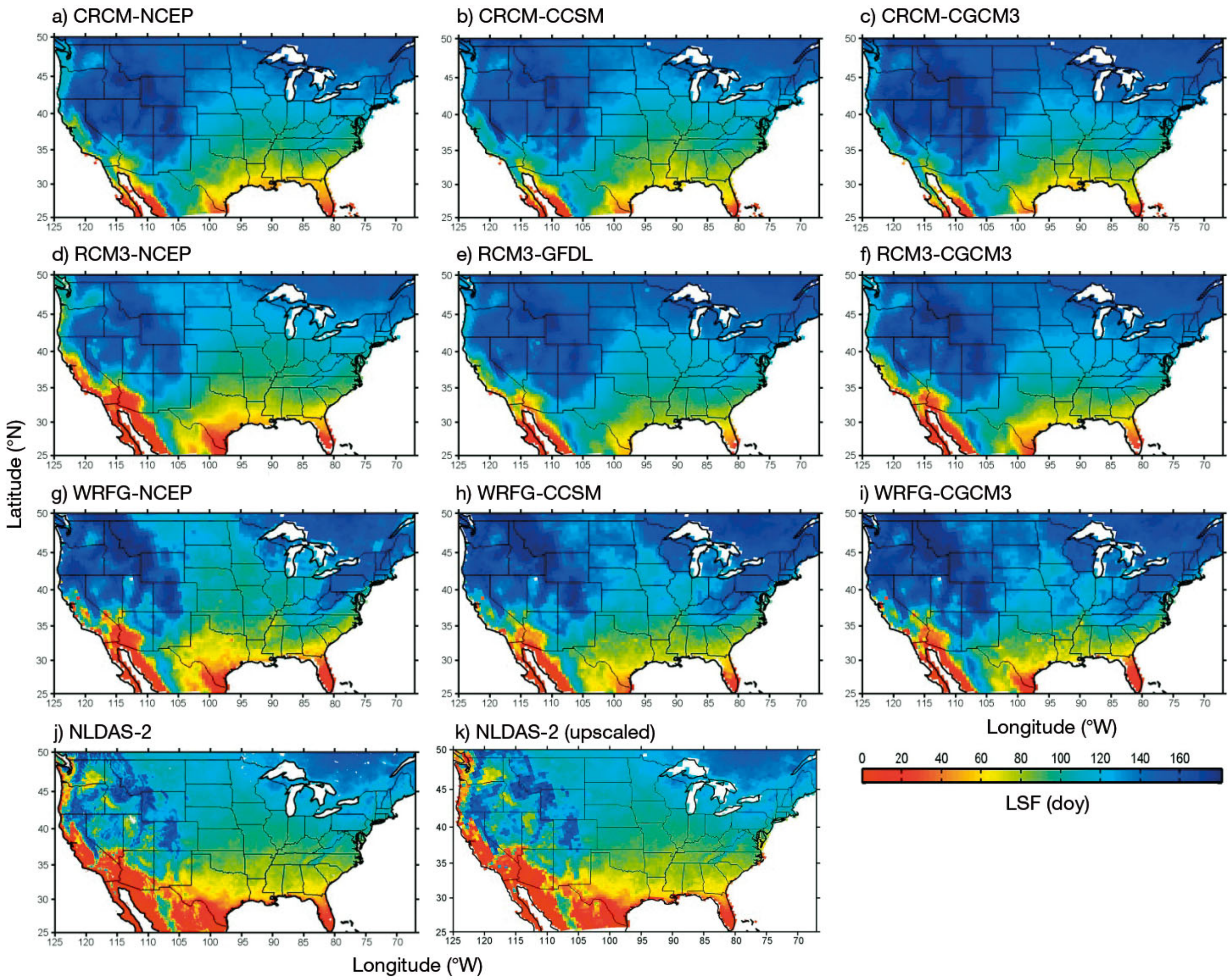

Fig. 2. The mean dates of the last-spring frost (LSF) for the perfect boundary condition simulations (RCM-NCEP) averaged over 1980–2004, for the baseline simulations (RCM-AOGCM) averaged over 1971–2000, and for the NLDAS-2 data averaged over 1980–2004 for the original NLADS-2 grid (labelled 'NLDAS-2') and the NARCCAP grid (labelled 'NLDAS-2 (upscaled)')

periods. To help quantify the spatial differences in the frost-free season indicators, we divide the study domain into 6 regions (Fig. 1d) following the divisions utilized in the reports by the US National Climate Assessment Program (Melillo et al. 2014). The 6 regions include the Pacific Northwest (42–49° N, 111–125° W), Southwest (31–42° N, 105–125° W), Midwest (37–49° N, 81–97° W), Southeast (25–37° N, 75–97° W), Northeast (37–49° N, 67–81° W) and Great Plains (25–42° N, 97–105° W and 42–49° N, 97–111° W). For each region and each indicator, we statistically compare the spatial patterns using the spatial correlation (r), normalized standard deviation, and centered root-mean-squared difference (RMSD) between the future and baseline periods. The resulting statistical measures are summarized in Taylor diagrams (Taylor 2001).

3. RESULTS

3.1. Frost-free season characteristics in the historical climates

To put the projected future changes of frost-free season indicators into historical context, we first focus on the historical climate period and compare the results from the baseline and perfect boundary condition simulations with those derived from the NLDAS-2 dataset for 1980–2004. For the comparison, the NLDAS-2 data are shown both in their original grid (1/8 degree, ~14 km) and also averaged from the original grid to the NARCCAP grid (50 km). Three frost-free season indicators averaged over the historical climate periods are compared including the date of last spring frost (Fig. 2), the date of the first autumn

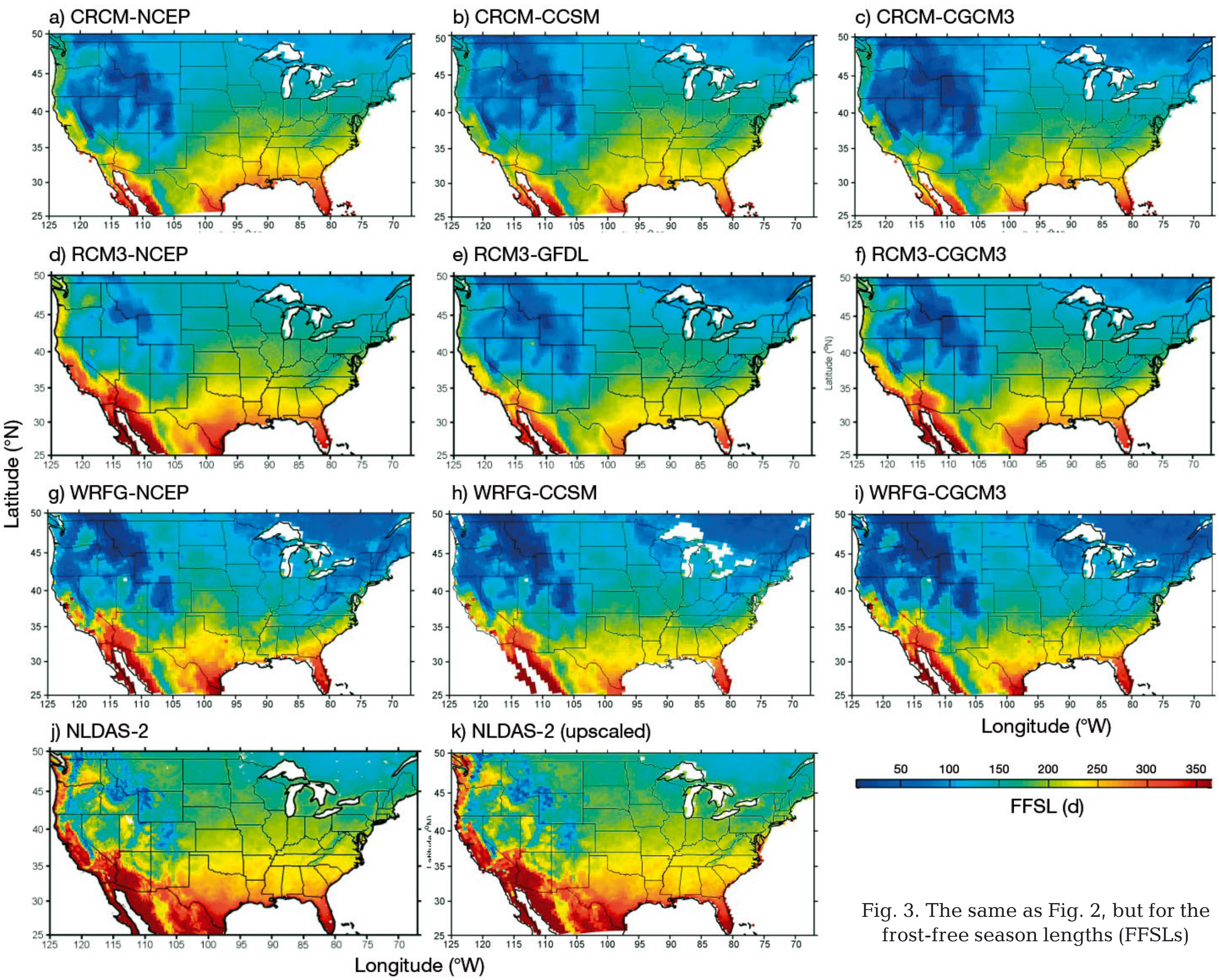

Fig. 3. The same as Fig. 2, but for the frost-free season lengths (FFSLs)

frost (Fig. S1), and the difference between the two or the length of the frost-free season (Fig. 3).

For all 3 indicators, both the perfect boundary condition and baseline simulations produce similar spatial patterns that are in good agreement with the observed spatial patterns. The spatial distributions, which largely reflect the influence of latitude, elevation, and oceans on minimum temperatures, show earlier (later) occurrences of the last spring (first autumn) frost and thus longer frost-free seasons in the southern states compared to the northern states, over coastal areas compared to interior lands, and over plains compared to mountains. The earliest occurrences of last spring frost are found in southern Florida, southern California, and along the coasts of the Gulf of Mexico and Gulf of California. The latest occurrences are seen over the high terrain of the Rocky Mountains and the Sierra Nevada (Fig. 2). This spatial pattern is reversed for the occurrences of first autumn frost (Fig. S1). The nearly opposite spatial patterns in the last spring and first autumn frost result in the longest frost-free season of >300 d along the Gulf of Mexico and Gulf of California, and the shortest frost-free season of <50 d over the Sierra Nevada, the Cascades and the Rockies (Fig. 3). On average, the frost-free season length ranges from 200–350 d in the Gulf States, the southwestern USA, and along the Gulf of California, to 150–200 d in the central Great Plains and the lower Midwest, 100–150 d in the upper Midwest, the Northeast, and the northern Great Plains, and <100 d at most of the high elevations of the western USA (Fig. 3). These values compare well to the observed frost-free season length as estimated by Sheffield et al. (2013) for North America from the gridded Hadley Center Global Historical Climatology Network dataset, and also to the season lengths calculated by McCabe et al. (2015) for 523 stations across CONUS.

Although the model combinations successfully capture the observed overall spatial pattern over the entire CONUS, all of them underestimate the spatial variability in the Northwest and the Southwest where topography plays a major role in regulating the frost-free season characteristics. This is evident when comparing the simulated and observed spatial distributions within these 2 regions, and is confirmed by considerably smaller spatial standard deviations for the simulated regional distributions compared to those in the NLDAS-2 distributions for the same regions. To quantify the differences between the models and the observations and between the models themselves, a regional mean and spatial standard deviation were calculated for each of the 6 regions (see Tables S2, S3 & S4). Across all 6 regions, the regional mean frost-free season lengths are considerably shorter in all the simulations compared to the observations with a combination of later (earlier) dates of the last spring frost (first autumn frost) in the simulations (Tables S2, S3 & S4). The results worsen from the perfect boundary condition simulations to the baseline simulations, as additional biases and errors associated with the AOGCMs are introduced into the baseline simulations through the lateral boundary conditions. Overall, the agreements between the simulated and the observed regional means and the spatial standard deviations are much better over the Southeast, the Northeast and the Midwest than over the Northwest, the Southwest and the Great Plains.

The considerably large differences between the simulations and NLDAS-2 data in the mountainous Pacific Northwest and the Southwest compared to the Great Plains and the Southeast cannot be simply explained by the difference in the NLDAS-2 and the RCM grid resolution. Many other factors contribute to the differences, including the failure of the terrain-following coordinate system used in all 3 of the RCMs to represent the horizontal pressure gradients near steep slopes (Zängl 2002) and the inadequacy of the boundary-layer and surface parameterization schemes used in the RCMs in describing local processes over complex terrains (Zhong & Chow 2013). A full explanation of the differences between the RCM results and the NLDAS-2 data would require comparisons of a large number of RCM simulations (e.g. varying resolution and parameterization schemes), which is beyond the scope of the current study. The readers are referred to Zhong & Chow (2013) for a summary of the various issues of regional models over complex terrain. The relatively poor agreement between the RCM simulations and the NLDAS-2 results over the Pacific Northwest and the Southwest calls for extra caution in interpreting the RCM projections of the frost-free season characteristics in these regions.

Comparing the perfect boundary condition simulations where the differences are introduced mainly by the RCMs (RCM-NCEP in Figs. 2 & 3; see Fig. S1 and Tables S2, S3 & S4), the results of CRCM and RCM3 are similar, and they are in closer agreement with observations than those of WRFG, with RCM3 slightly outperforming CRCM (Tables S2, S3 & S4). A similar conclusion can be drawn when comparing the 6 baseline simulations. Of all the model combinations, RCM3-CGCM3 appears to yield the best overall agreement with observations when considering all 6 regions and the 3 indicators. The 2 baseline simulations with WRFG produce the least agreement, with WRFG-CGCM3 being slightly worse. The results appear to be more similar when the same RCM is nested within different AOGCMs (e.g. CRCM-CCSM vs. CRCM-CGCM3) than when different RCMs are nested within the same AOGCM (e.g. CRCM-CGCM3 vs. RCM2-CGCM3).

3.2. Potential changes in frost-free season characteristics by mid-century

The potential changes in the 3 frost-free season indicators are determined by subtracting the simulated baseline climate from the projected future climate for each of the 6 RCM-AOGCM combinations (Figs. 4, 5 & 6). Although the baseline simulations underestimate the frost-free season lengths by simulating later (earlier) dates of the last spring (first autumn) frost, we assume that biases of similar nature are carried by the RCM-AOGCM combinations to the future climate simulations, so that the differences between the future climate period and the baseline period are good indicators of changes in mean climate conditions.

For the last spring frost (Fig. 4), the differences for all model combinations are negative nearly everywhere, with the exception of a very few isolated positive values for RCM3-GFDL, indicating that the last spring frost is likely to occur earlier over CONUS in the future climate. The average over the 6 model combinations (i.e. the ensemble average, Fig. 4g) suggests a shift of 5 to 15 d across most of the USA, except for some areas along the Pacific Coast where the shift is >25 d. The ensemble spread (Fig. 7a) is generally <15 d, with a larger spread over the northern Great Plains and along the Pacific Coast. Comparison of the individual simulations suggests that both the RCMs and the AOGCMs are contributing to differences among the ensemble members. Averaging over the entire CONUS, WRFG-CGCM3 has the

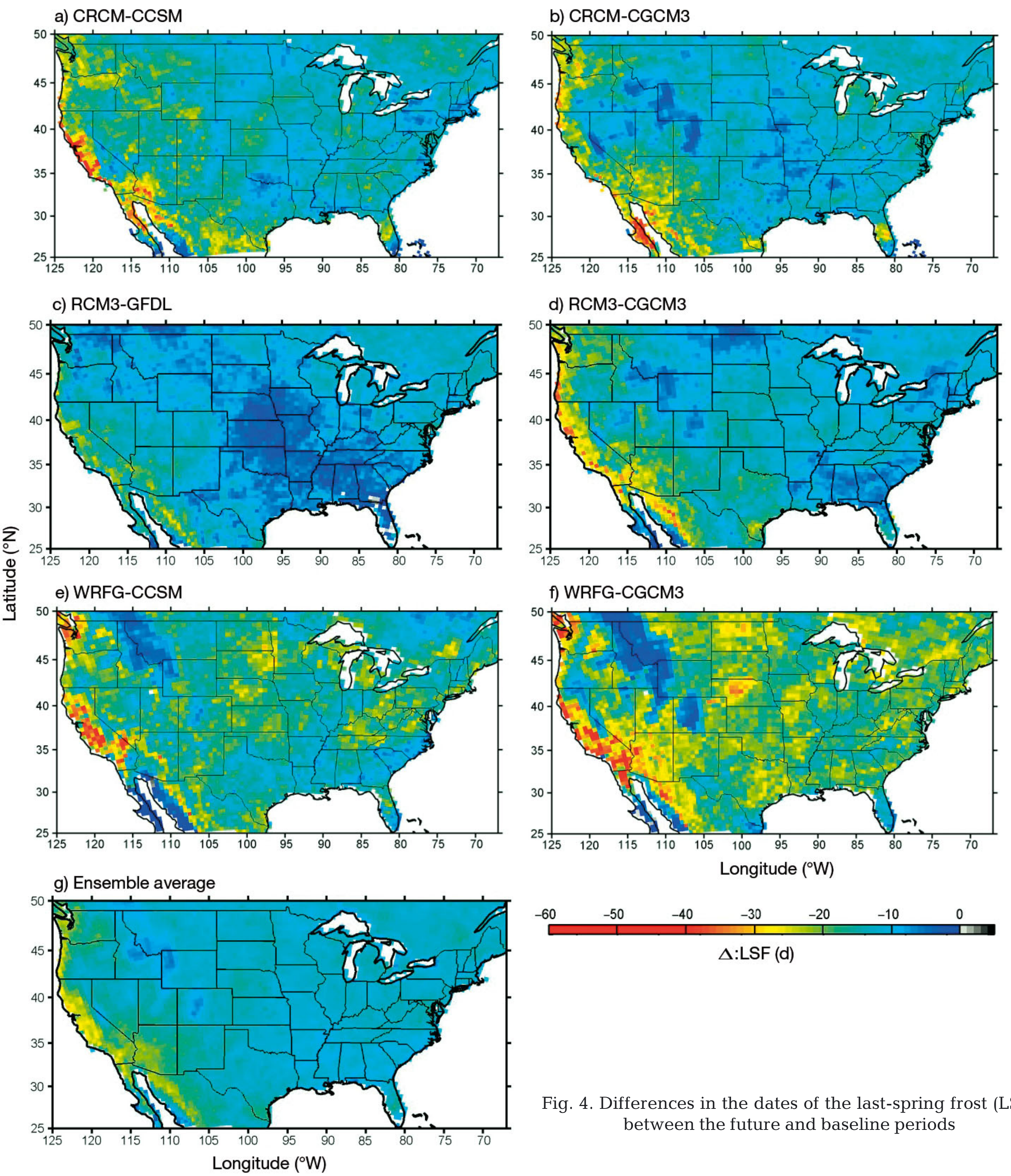

Fig. 4. Differences in the dates of the last-spring frost (LSF) between the future and baseline periods

largest overall change of −17.3 d, followed by WRFG-CCSM with −14.5 d (Table 1). The larger overall changes with WRFG are the result of larger changes almost everywhere except for some areas of the Rocky Mountains, where the changes projected by WRFG are smaller than those of the other models. The smallest domain-average change of −8.5 d is projected by RCM3-GFDL, which shows almost no change or even a slight delay of a few days in extreme southeastern Louisiana and the Florida Peninsula. However, the domain average for RCM3 when driven by CGCM3 is considerably larger (−12.7 d), due mostly to differences between the RCM3-GFDL and RCM3-CGCM3 projections along the west coast and in the Great Plains. In contrast, the domain averages for the CRCM-CCSM and CRCM-CGCM3 sim-

Table 1. The overall mean changes in the dates of the last spring frost (LSF), first-autumn frost (FAF), and frost-free season lengths (FFSL) between the future (2041–2070) and the baseline (1971–2000) climate periods averaged over the entire USA

	ΔLSF (d)	ΔFAF (d)	ΔFFSL (d)
CRCM-CCSM	−14	16	30
CRCM-CGCM3	−13	17	30
RCM3-CGCM3	−13	16	29
RCM3-GFDL	−9	11	20
WRFG-CCSM	−15	14	28
WRFG-CGCM3	−17	8	26

ulations differ by only 1 d, and the spatial patterns of the projected changes in last spring frost are similar.

The opposite change is projected to occur for the first autumn frost (Fig. 5). Projections from all but 1 RCM-AOGCM combination indicate a delay in the first autumn frost across the entire domain, with the ensemble average (Fig. 5g) suggesting changes ranging from 1 to 20 d in the eastern and central USA and 20 to 35 d in areas of the western USA. One member of the ensemble, WRFG-CGCM3, has a slight shift of up to 10 d towards an earlier first autumn frost in some areas of the Great Plains and the Midwest. But the same model combination also produces the longest delay in the coastal areas of the Northwest. In contrast, the WRFG simulation driven by CCSM projects a delay in the first autumn frost across the entire CONUS (although, similar to the WRFG-CGCM3 simulation, the largest delay occurs along the coastal Northwest). This difference is evident in the considerably larger domain average for WRFG-CCSM compared to WRFG-CGCM3 (13.6 d versus 8.4 d). The CRCM-CCSM, CRCM-CGCM3, and RCM3-CGCM3 simulations have similar domain averages (16.0, 17.0, 16.1 d, respectively), and all project the largest delays in first autumn frost to occur in the Rocky Mountains from northwestern Montana to western Colorado and in the Sierra Nevada. None of these simulations project the large changes in the Pacific Northwest as seen for the WRFG simulations. In contrast to the other simulations, the RCM3-GFDL simulation projects a relatively uniform change in the date of last-autumn frost of approximately 11 d, on average, across CONUS. Compared to the last spring frost, the ensemble spread for the first autumn frost (Fig. 7b) is considerably larger over the Northwest and the Southwest, especially over the high mountain ranges (Rockies, Sierra Nevada and the Cascades) where the spread can be larger than the projected mean changes.

The change towards an earlier occurrence of the last spring frost and a later occurrence of first autumn frost leads to a lengthening of the frost-free season in the future (Fig. 6). The variability is small spatially and among the model combinations in the central and eastern USA, with values of 10 to 40 d, and large in the western USA where the values can change quickly from a few to 60 or even 90 d in a short distance (Fig. 6g). The largest increase of 99 d is projected by WRFG-CGCM3 over the Washington coast (Fig. 6f). The ensemble average shows an increase of a few days up to about 3 wk across most of the USA, except for areas of high terrain in the western USA where the increases can be a month or longer. These areas of high terrain also have the largest ensemble spread (Fig. 7c). Despite the large spatial variability in the western USA, the average increase in the frost-free season length across the entire USA is very close (26–30 d) among 5 out of the 6 model combinations (Table 1). The exception is RCM3-GFDL, which yields an average increase of 20 d resulting from smaller changes nearly everywhere across the domain along with weaker spatial gradients.

The range of the projected changes from the 6 model combinations of the NARCCAP ensemble provides a preliminary estimate of the uncertainty surrounding the future values of the frost-free season indicators (Fig. 7). The uncertainty in the projected frost-free season length (Fig. 7c) is substantial, varying from 20 to 30 d in much of the central and southeastern USA, to more than 30 d over most of the western USA, and to more than 70 d in the Cascades, the northern and central Rockies, and the Sierra Nevada. Only in the north-central and northeastern USA does the uncertainty range fall below 20 d. Over much of the eastern USA, uncertainty surrounding the advance in the date of last spring frost is the greater contributor to the uncertainty in the frost-free season length compared to the uncertainty surrounding the delay in first autumn frost. This is also the case for the southwestern USA, including Arizona and coastal and central California. Elsewhere in the western USA, but particularly in the mountainous areas, uncertainty surrounding the delay in the first autumn frost is much greater than uncertainty in the advance of the last spring frost.

The lengthening of the frost-free season results from a combination of the advance in the last spring frost and the delay in the first autumn frost. However, the amount of lengthening is not symmetric in the spring and autumn, and the relative contributions from the advance in spring or the delay in autumn to the frost-free season length increase vary considerably by region and by model (Fig. 8). Over the north-

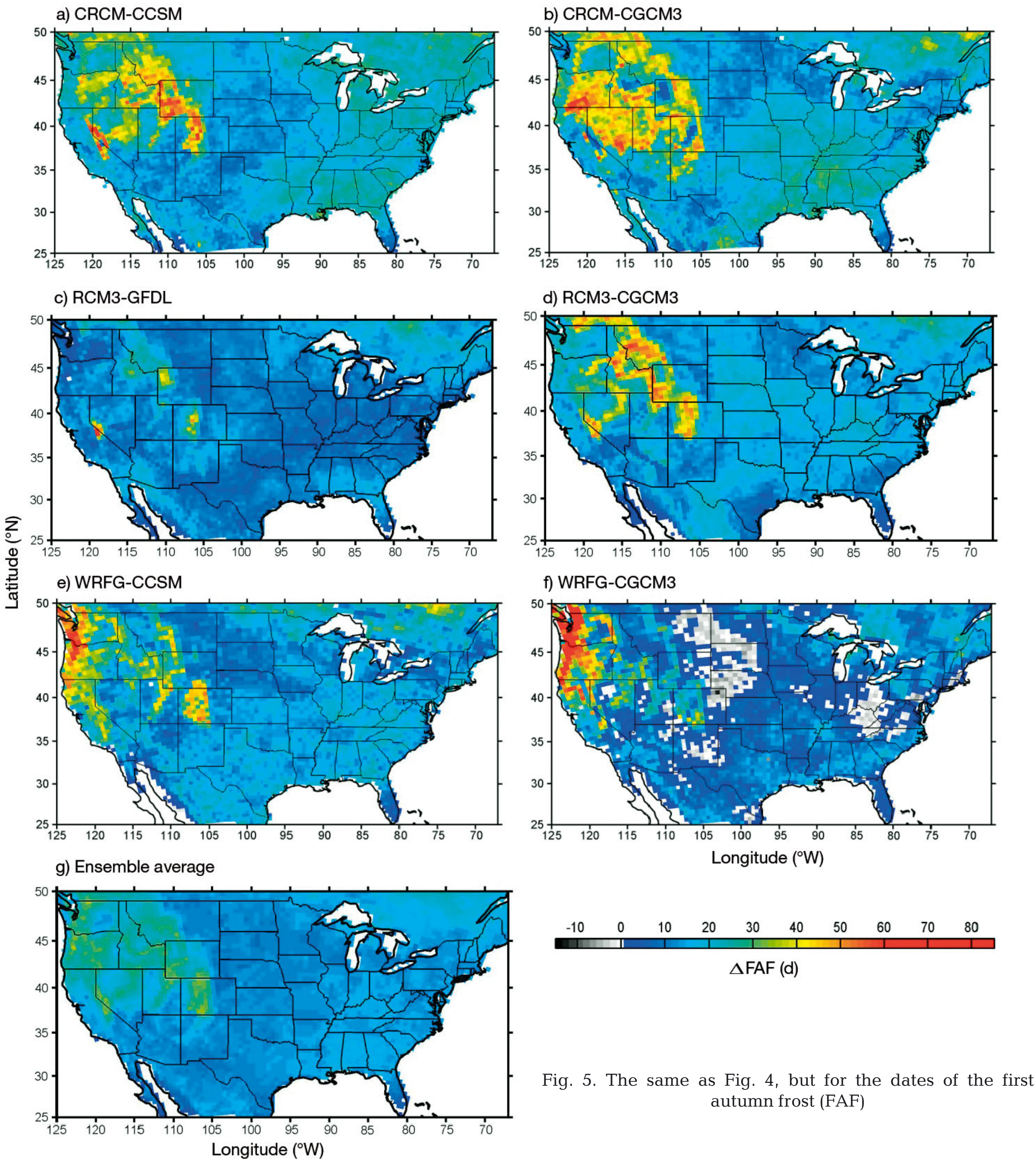

Fig. 5. The same as Fig. 4, but for the dates of the first autumn frost (FAF)

ern Great Plains, the Midwest, and the Northeast, the asymmetry is relatively small in magnitude and variable in spatial pattern among 4 of the 6 RCM-AOGCM simulations. The 2 WRFG simulations, however, show considerable asymmetry across the central and eastern USA, with advance in the last spring frost accounting for 60 to 90 % of the increases in the frost-free season length. The ensemble members are in agreement that the advance in the last spring frost date will be greater than the delay in the first autumn frost date over California and portions of the Southwest. Elsewhere in the western USA, especially over high terrain, all ensemble members are in agreement that the contribution from the delay in the first autumn frost contributes more to the lengthening of the frost-free season.

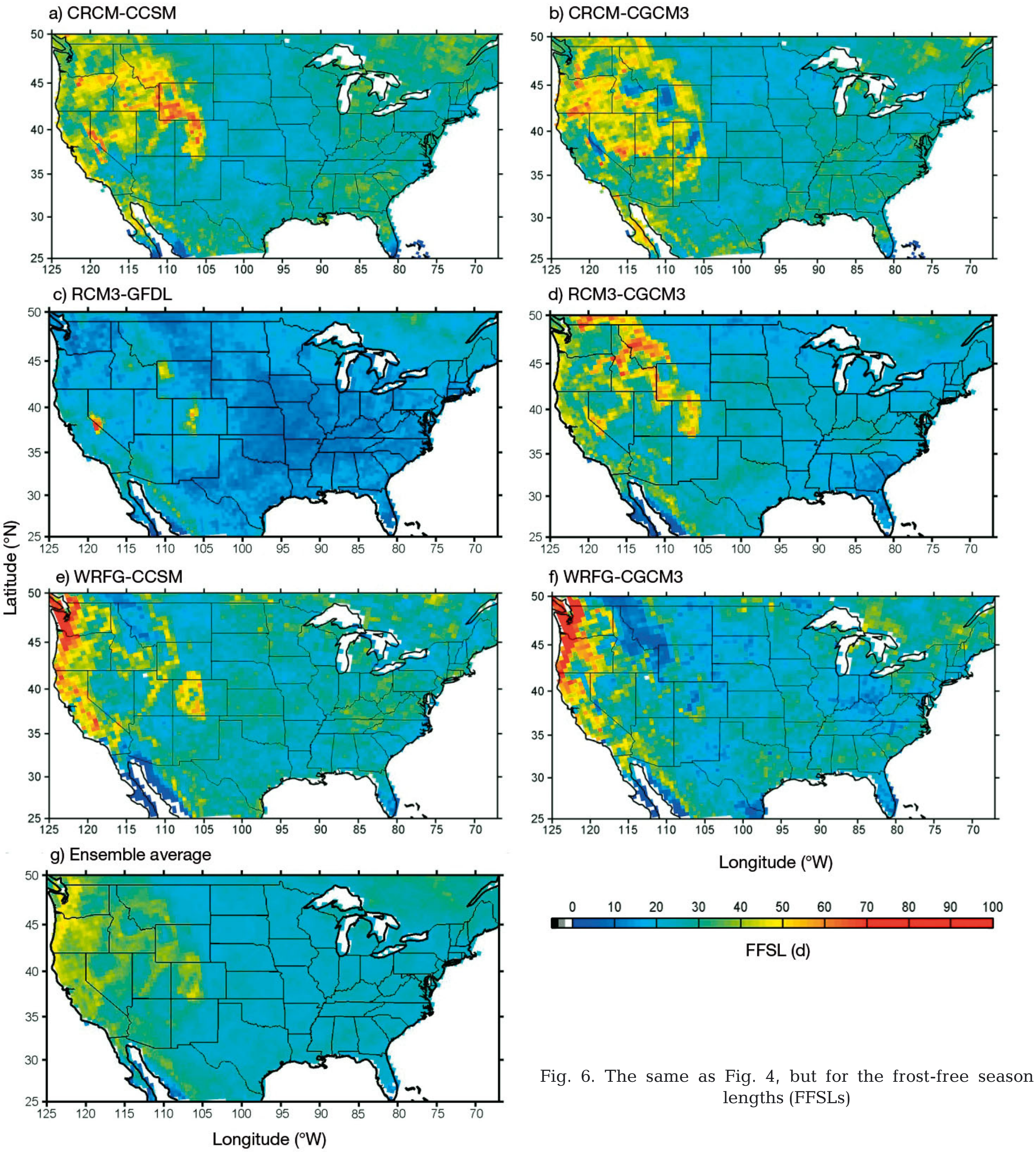

Fig. 6. The same as Fig. 4, but for the frost-free season lengths (FFSLs)

3.3. Statistical analysis of the spatial patterns of the frost-free season indicators

To determine to what degree the spatial patterns of the 3 frost-free season indicators differ between the baseline and the future periods, we generated Taylor diagrams (Taylor 2001) that quantify the degree of spatial correspondence in terms of 3 statistics: the spatial correlation (r), the centered root-mean-square deviation (RMSD), and the ratio of the spatial standard deviation (σ_f:σ_b), also referred to as the normalized standard deviation, between the future (subscript f) and baseline (subscript b) periods. A higher r and a smaller RMSD indicate a closer match in spatial patterns between the 2 periods and the ratio σ_f:$\sigma_b \approx 1$ indicates that the pattern variations are of similar am-

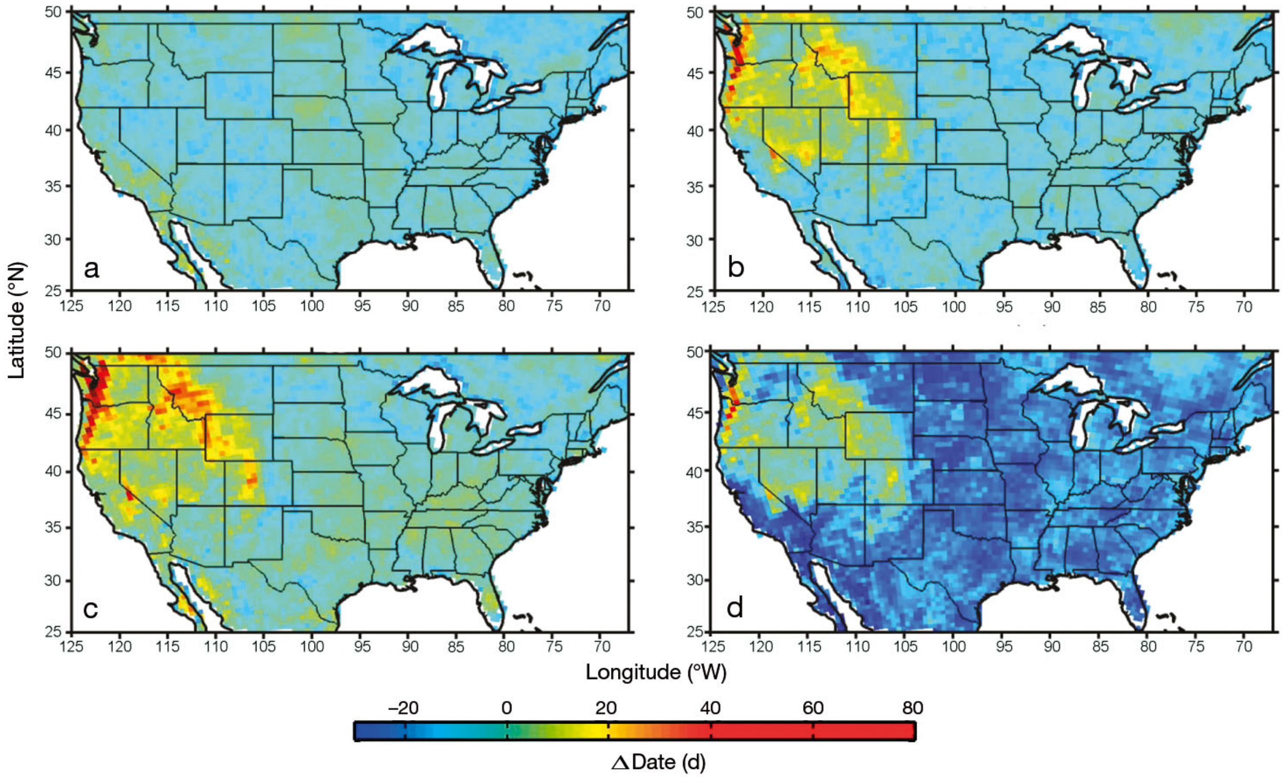

Fig. 7. The ensemble spread of the differences in the dates of the (a) last spring frost (LSF), (b) first autumn frost (FAF), and (c) frost-free season lengths between the future and the baseline climate periods, and (d) the differences in the spread between the date of the FAF and date of the LSF (b minus a)

plitude in the 2 periods. Future patterns that agree well with the baseline patterns will lie nearest to the reference point indicating a perfect match at (r = 1, RMSD = 0, σ_f:σ_b = 1). The statistical analysis was performed separately for each of the previously defined 6 regions (Northeast, Southeast, Midwest, Great Plains, Southwest, and Northwest), and a Taylor diagram was generated for each region and each index.

For the Great Plains, the combination of very high spatial correlations r ≈ 0.99, normalized standard deviation values close to unity, σ_f:σ_b ≈ 1, and very small RMSD values of all data points in the Taylor diagrams (Figs. 9c & 10c; Fig. S2c) indicate that the spatial distributions of all 3 frost-free season indicators for the baseline and future periods are nearly identical, varying only in terms of the regional mean.

Spatial correlations are somewhat lower (0.96 < r < 0.99) for the neighboring Midwest region (Figs. 9d & 10d, Fig. S2d). For the date of last spring frost (Fig. 9d), all data points are clustered around the arc with σ_f:σ_b = 1, indicating similar amplitude in pattern variation around the regional mean between the future and baseline periods. However, for the date of first autumn frost (Fig. S2d), and to a lesser extent the frost-free season length (Fig. 10d), the spatial pattern variations are greater (σ_f:σ_b > 1) in the future period for 2 of the ensemble members (RCM3-CGCM3 and CRCM-CGCM3) and smaller (σ_f:σ_b < 1) for the other 4 ensemble members.

In the Southeast region, the pattern differs little between the baseline and future periods for the date of last spring frost, as all data points are near the reference point (r = 1, RMSD = 0, σ_f:σ_b = 1) (Fig. 9e). The differences are larger for the date of first autumn frost, with smaller r and σ_f:σ_b < 1 for all but 1 (RCM3-GFDL) ensemble member (Fig. S2e), indicating somewhat smaller amplitude of spatial variations in the future period compared to the baseline period. The spread among the data points is also larger. Similar differences are found for the frost-free season length (Fig. 10e).

In the Northeast, the spatial variations are systematically smaller for the date of last autumn frost and frost-free season length, as the data points from all ensemble members show σ_f:σ_b < 1 (Fig. 10f, Fig. S2f). The difference in the date of last spring frost results mostly from the 2 CGCM3-driven simulations, with CRCM-CGCM3 producing σ_f:σ_b < 1 while WRFG-CGCM3 yields σ_f:σ_b > 1. The 2 simulations also have smaller r compared to the other simulations.

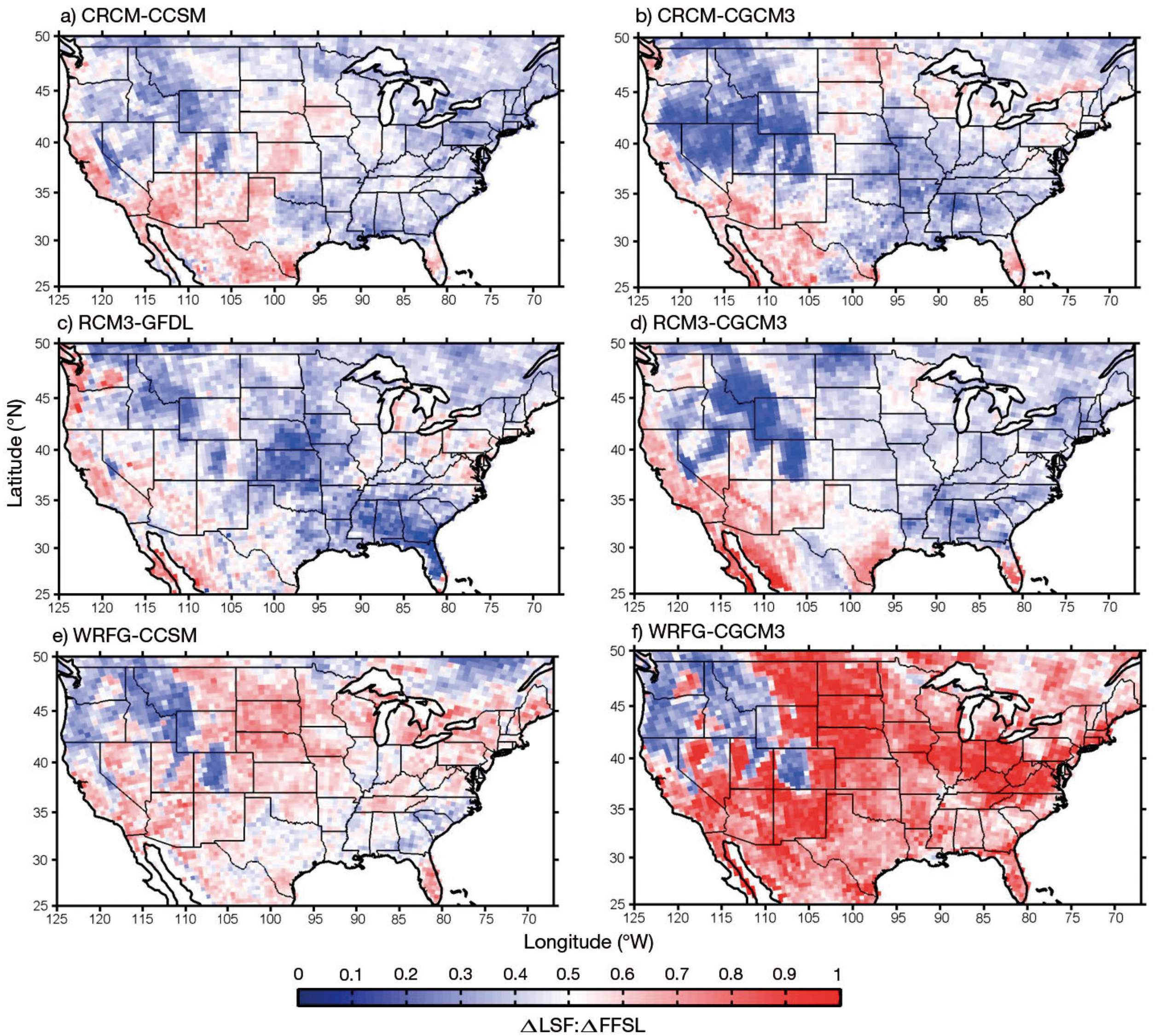

Fig. 8. The ratio of the differences (future minus baseline) in the dates of the last spring frost (ΔLSF) to the differences in the frost-free season length (ΔFFSL)

In contrast to the Southeast and Northeast, the future spatial variations in the date of first autumn frost appear to have somewhat larger amplitude in the Southwest, as all data points show $\sigma_f:\sigma_b > 1$ (Fig. S2b). The opposite is true for the date of last spring frost as $\sigma_f:\sigma_b < 1$ for all data points (Fig. 9b). The differences of opposite nature balance out, resulting in a close match in the spatial patterns of the frost-free season length between the baseline and the future periods, as indicated by the close proximity of all the data points to the reference point (Fig. 10b).

Finally, the statistics for the Northwest region suggest the greatest deviations in the spatial patterns between the future and baseline periods for all 3 indicators (Figs. 9a & 10a, Fig. S2a). The spread among the data points is also the largest among the 6 regions with the 2 WRFG simulations standing out as having the lowest r and largest $\sigma_f:\sigma_b$ and RMSD values. For the date of the last spring frost (Fig. 9a), the spatial correlations for four of the ensemble members are approximately 0.98, but lower correlations of 0.93 to 0.95 are evident for the 2 WRFG simulations. The normalized standard deviation ($\sigma_f:\sigma_b$) is >1 for all ensemble members, especially for the 2 WRFG simulations that have $\sigma_f:\sigma_b > 1.5$, suggesting that the future pattern will have much larger variations around the regional mean. The 2 WRFG simulations also differ substantially from the others for the date of the first autumn frost, with lower correlation (0.88, 0.93 compared to 0.95–0.99 in the other simulations), larger RMSD (0.42, 0.64 compared to 0.24–0.36) and

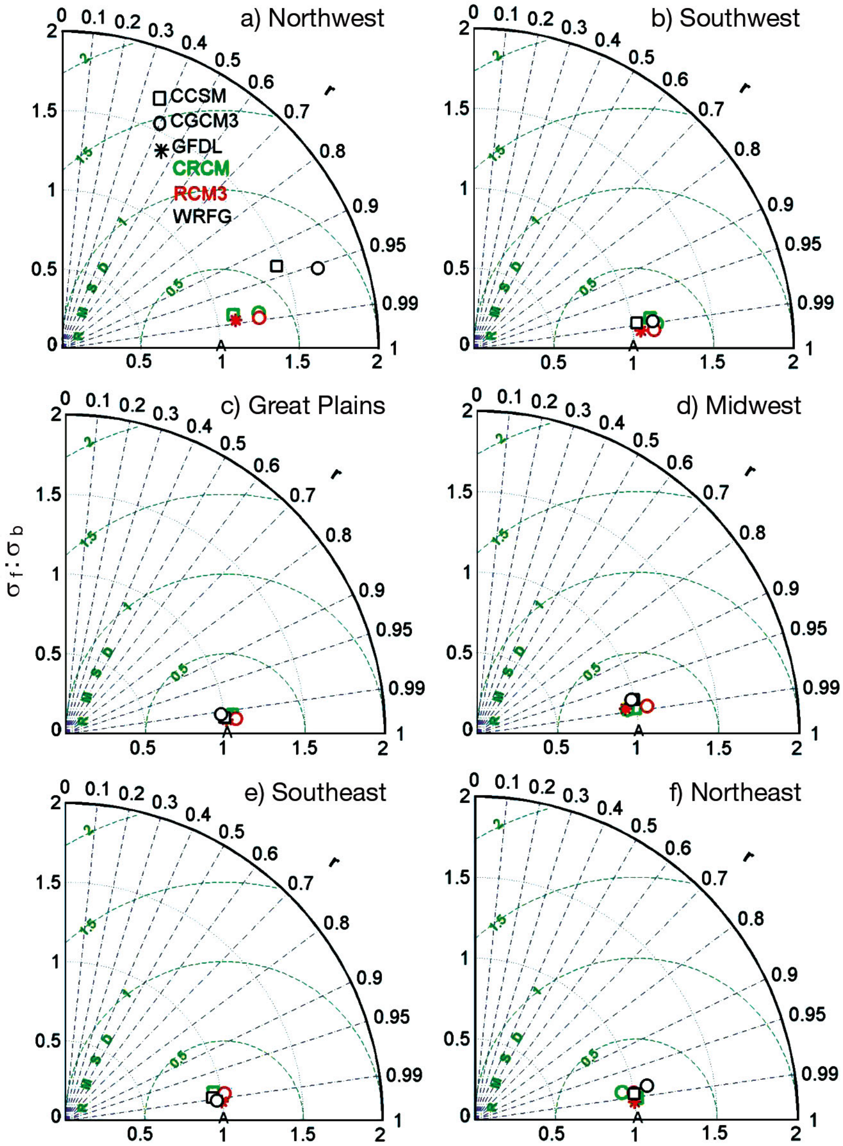

Fig. 9. Taylor diagrams for the dates of the last-spring frost in each of the 6 regions shown in Fig. 1d. The metrics shown are computed by comparing the spatial patterns of the dates of the last-spring frost averaged over the future and the baseline climate periods in each region from each simulation. They are the spatial correlation coefficient r (shown by the azimuthal angle); normalized standard deviation σ_f:σ_b (horizontal and vertical axes), with subscript f indicating future and b indicating baseline (shown by the radial distance from the origin), and centered root-mean-squared difference RMSD, (shown by the distance from the reference point A on the *x*-axis defined as r = 1, σ_f:σ_b = 1, RMSD = 0) between the future and baseline periods. Symbols: driving AOGCM; color: RCM used

higher normalized standard deviations (1.12, 1.31 compared to 0.72–0.84) (Fig. S2a). Consequently, the statistics from the 2 WRFG simulations suggest that the spatial patterns of the frost-free season length will differ significantly between the future and the baseline periods (Fig. 10a). However, for the other 4 simulations, the increase (σ_f:σ_b > 1) in the amplitude of spatial variations for the last spring frost date and the decrease in the amplitude (σ_f:σ_b < 1) for the first autumn frost date between the future and the baseline periods partially cancel each other out, bringing σ_f:σ_b closer to 1 (Fig. 10a).

4. DISCUSSION

As shown above, the NARCCAP models projected a larger increase in the frost-free season length in the western USA compared to the central and eastern USA, which is in good agreement with that of recent observed trends in frost-free season length. For example, Walsh et al. (2014) and Easterling (2002) found that the observed trend in the lengthening of the frost-free season is twice as large for the Northwest and Southwest compared to elsewhere in CONUS. There are also broad similarities with the projected changes in the multi-model mean of frost-free season length for the late century (2081–2100) obtained from an ensemble of 14 CMIP5 models run under the RCP8.5 greenhouse gas emissions scenario (Maloney et al. 2014). As for the NARCCAP simulations, the multi-model mean of the CMIP5 projections suggests greater increases in season length in the western rather than eastern USA, but the spatial pattern is much smoother illustrating the advantage of using higher-resolution dynamically downscaled simulations in assessment studies.

The current results reveal considerable differences in the spatial patterns of the projected changes among the RCM-AOGCM combinations, despite the broad agreement on the sign of the future changes in the frost-free season indicators and the domain-averaged values. The large spread among the simulations, an indication of large uncertainties, highlights the significant challenges faced by policy makers in assessing local climate change impacts and designing adaptation strategies in these regions. This uncertainty also

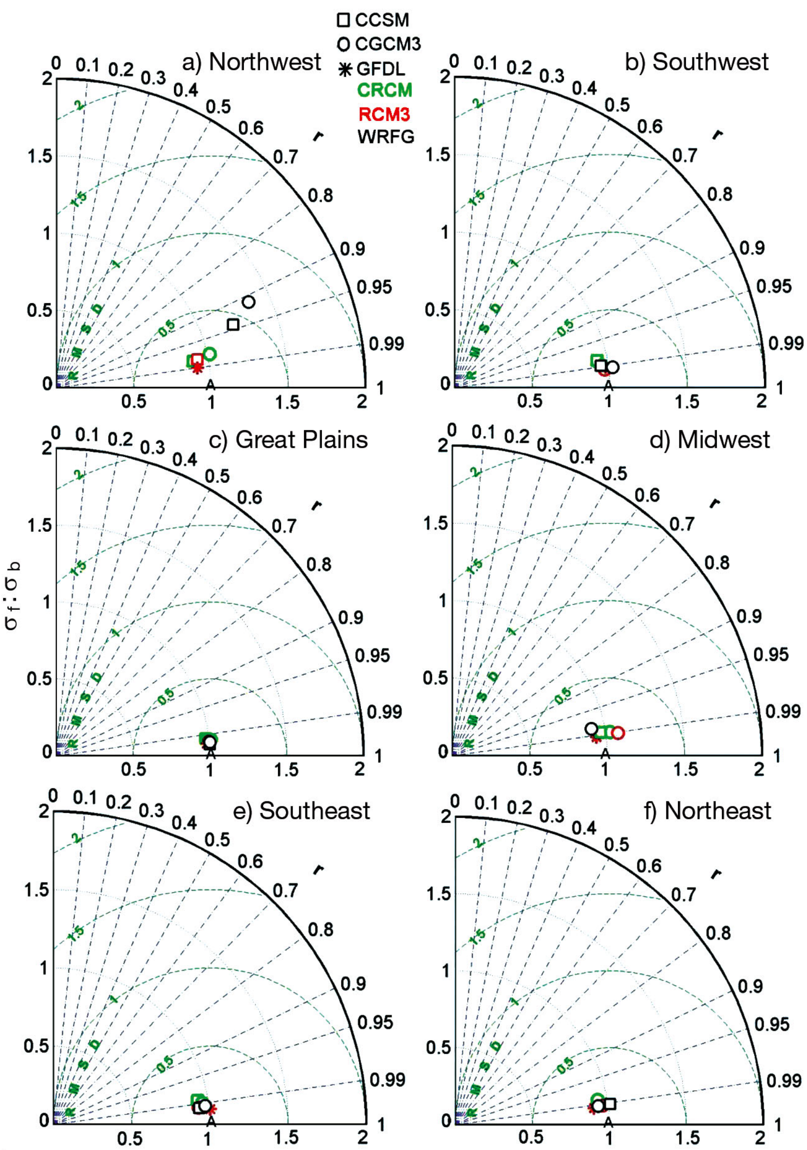

Fig. 10. The same as Fig. 9, but for the frost-free season lengths

terrain processes (Zhong & Chow 2013) as well as the potential usefulness of further downscaling and debiasing using empirical methods for variables that are strongly influenced by local conditions.

Our analyses also address the potential asymmetry in the lengthening of the frost-free season. The observed greater advance of the last spring frost date compared to the delay in first autumn frost during the 20th and early 21st centuries has been attributed to changes in surface conditions and boundary-layer processes, in addition to greater warming in the spring than in autumn (Linderholm 2006, Barichivich et al. 2012). Christidis et al. (2007) argue that earlier snow melt enhances springtime warming, further advancing the date of the last spring frost. Both Barichivich et al. (2012) and Christidis et al. (2007) have inferred that the lengthening of the frost-free season should become more symmetrical in the future, as continued warming delays the date of first autumn frost. In the eastern and central USA, a relatively symmetrical lengthening is indeed portrayed by the majority of the NARCCAP ensemble members, with the exception of the 2 WRFG simulations that have a larger advance of the last spring frost date. The potential asymmetry of the seasonal lengthening is much more complex in the western USA. The advance in the last spring frost date contributes more to the lengthening of frost-free season than the delay in the first autumn frost date in California and parts of the Southwest, but elsewhere in the western USA, especially over regions of high terrains, longer lengthening is found in autumn than in spring. These differences in seasonal asymmetry are not easily explained by the differences in the projected changes in autumn versus spring minimum temperatures, and we suspect, following Christiansen et al. (2011), that simulated earlier snowmelt in the mountainous areas of the western USA contributes to reduced soil moisture, further warming, and greater delays in the first autumn frost date in the model simulations. Between-model differences in the altitude of the pro-

points to the potential pitfalls of relying primarily on multi-model means for planning and decision-making. The inter-model spread of the frost-free season length is greatest in the mountainous areas of the western USA. For example, while most of the RCM-AOGCM combinations show a relative maximum in the increase of the frost-free season length over the high terrain of the Rockies and the Sierra Nevada, CRCM-CGCM3 has a relative minimum at these high elevation locations. Another example of model differences is the projected lengthening in the Cascades, which varies from 10–20 d for RCM3-GFDL to 70–90 d for WRFG-CGCM3. The much larger uncertainty in the mountainous West points to a need to improve the ability of RCMs in simulating complex jected greatest reductions in seasonal snow cover could help explain why some of the NARCCAP simulations project the largest changes in the date of first autumn frost at the highest elevations of the Rocky Mountains, whereas others project the largest changes at lower elevations. This interpretation is consistent with the observation of Feng & Hu (2004) that, during the 1951–2000 period, the dates of last spring frost remained unchanged at the higher elevations of the Rocky Mountains. The suggestion of relatively small future asymmetry of the frost-free season lengthening in the eastern and central USA from the NARCCAP simulations is in contrast with the aforementioned analysis of the multi-model mean of the CMIP5 simulations for the end of the century (Maloney et al. 2014), which suggests that changes in the last spring frost date will be greater than those in the first autumn frost date across North America. The NARCCAP simulations project a more complex spatial pattern in the level of symmetry of the lengthening of the frost-free season.

The statistical analyses of the spatial patterns of the projected changes in the frost-free season indicators also provide some insights on possible alterations of the major climate factors controlling minimum temperature and frost occurrence for different regions of the USA. Latitude, elevation, and coastal influences are stable factors between the historical and future periods, but surface conditions and boundary-layer processes, and the frequency and timing of synoptic and sub-synoptic-scale circulations conducive to frost can vary in a future climate. For the Great Plains, we interpret the very good spatial correspondence for all the NARCCAP models as an indication that the influence of latitude dominates the spatial distributions of the indicator variables in this region for both time periods, which is a reasonable interpretation given the greater north–south extent of this region and the modest variations in elevation. The spatial statistics also suggest little future change in the pattern and amplitude of the spatial variations of the frost-free season indicators across the Southeast, where distance from the Gulf Coast in addition to latitude influences the spatial gradients. On the other hand, for the Northeast and Southwest, the amplitude of the deviations around the spatial mean in the future period increases (decreases) for last spring frost date (first autumn frost date) for most RCM-AOGCM combinations. This suggests within-region differences in future surface conditions and/or circulation may be equally as important as latitudinal, elevation, and coastal influences. Inter-model differences confound the interpretation for the Midwest and Northwest regions. This is especially the case for the Northwest where the smaller spatial correlations, larger RMSD and normalized standard deviation values for the 2 WRFG simulations suggest that the future spatial patterns of the frost-free season indicators will deviate substantially from those of the baseline period. On the other hand, the other 4 simulations suggest that changes in surface conditions and/or circulations could lead to reduced spatial variability in the frost-free season indicators. This interpretation is consistent with hydrological changes resulting from earlier snowmelt in mountainous regions, leading to both the advance of last spring frost date and a delay of first autumn frost date in the mountainous regions to dates comparable with those at lower elevations within the region. However, model biases may also be contributing to the projected changes in areas of complex topography. For example, Salzmann & Mearns (2012) found that for the perfect boundary condition simulations, CRCM and RCM3 were generally both too dry and too warm and simulated a too short a period of snow cover in the Upper Colorado River Basin (WRFG was not included in their analysis).

It is necessary to note that the results presented here are for the A2 greenhouse gas emissions scenario, which assumes that greenhouse gas emissions will continue to grow (Nakičenovič et al. 2000). Thus, the projected changes will likely be smaller for the more balanced emissions scenarios. Furthermore, the 50 km resolution of the NARCCAP simulations is insufficient to fully capture spatial variations in the frost-free indicators, especially in areas of complex topography, and further dynamical or empirical downscaling may be needed for some applications. Another consideration is the influence of the size of the ensemble on the uncertainty range. Obviously, small ensembles are likely to have a narrower uncertainty range than those with a larger number of members. Ideally, dynamically downscaled simulations would be available for each of the global models in the CMIP archive. However, the large resources needed for dynamical downscaling confines these efforts to only a small number of AOGCMs. The choice of AOGCM also influences the uncertainty range, and, in the case of the NARCCAP simulations, the range of the annual and seasonal temperature changes projected by the CMIP3 models used to drive the NARCCAP simulations is smaller than the range for all CMIP3 models (Kunkel et al. 2013g). From this, we infer that a different selection of AOGCMs in the NARCCAP experimental design would have led to a larger uncertainty range for the frost-free season characteristics. Also, NARCCAP employed AOGCM simulations from the CMIP3 archive rather than the more recent CMIP5 archive (Taylor et al. 2012) that contains a larger ensemble of more advanced models, although the uncertainty remains large for the CMIP5 ensemble (Knutti & Sedlá ek 2013). In spite of these limitations, the range of projected changes in the frost-free season characteristics obtained from the NARCCAP simulations is large, especially for the mountainous West, and provides stakeholders with insights into complex system behavior and helps them to critically evaluate adaptation options, hopefully leading to robust decision making. Furthermore, at the time of this study, the NARCCAP simulations were the only suite of dynamically downscaled climate simulations for North America that were easily accessible, had sufficient resolutions for climate impact assessments, and provided a range of projected future conditions (Mearns et al. 2015).

In sum, we have provided an evaluation of the date of last spring frost, date of first autumn frost, and length of the frost-free season as projected by the suite of NARCCAP dynamically downscaled climate simulations for the mid-21st century. The focus was on the uncertainty revealed by the range of simulations so that this uncertainty can be incorporated into robust climate change adaptation decision making. In addition, the analyses reveal a number of interesting questions for further research on inter-model differences in the boundary-layer and surface processes contributing to changes in the frost-free season, particularly in areas of complex topography.

5. CONCLUSION

In this study, we investigated the effect of increasing atmospheric greenhouse gas emissions on frost-free season indicators over CONUS using archived daily minimum temperatures from a 6-member NARCCAP RCM-AOGCM ensemble for historical and mid-century climate periods.

The multi-model mean projects a shift across the USA towards earlier occurrences of last spring frost and later occurrences of first autumn frost, which together lead to increases in the frost-free season length. Averaging over the entire country, the projected increases in the frost-free season length are very consistent (26 to 30 d) among 5 out of the 6 RCM-AOGCM combinations, with 1 combination (RCM-GFDL) projecting a shorter average increase of 20 d. The multi-model mean increase in frost-free season length varies from approximately 15 to 30 d over the central and eastern USA to approximately 30 to 55 d over the western USA.

Despite the broad agreement on the sign of the future changes in the frost-free season indicators and the domain-averaged values, there are considerable differences in the spatial patterns of the projected changes among the simulations and large inter-model spread. The inter-model spread, an indication of uncertainty, is greatest in the mountainous areas of the western USA, exceeding 70 d in the projected changes in the frost-free season length in the Cascade Mountains of Washington and Oregon, the northern Rocky Mountains from western Montana to central Colorado, and parts of the Sierra Nevada. The uncertainty surrounding the date of first autumn frost is the major contributor to the high uncertainty in the projected frost-free season length for these mountainous areas. This is in contrast to other regions, especially the Great Plains, where the inter-model spread in last spring frost date contributes more to the frost-free season length uncertainty, although the overall uncertainty in frost-free season is much lower compared to the western mountainous areas.

In the eastern and central USA, a relatively symmetrical lengthening is projected by the majority of the NARCCAP ensemble members. The asymmetry of the seasonal lengthening is much more complex in the western USA. For most of California and portions of the Southwest, the model simulations are in agreement that the advance in the last spring frost date will be greater than the delay in the first autumn frost date. Elsewhere in the western USA, especially over regions of high terrain, there is fairly good agreement that the frost-free season will lengthen more in autumn than spring.

Acknowledgements. The manuscript was informed by research activities funded by the National Science Foundation (Award CNH 0909378), US Forest Service – Northern Research Station under Research Joint Venture Agreement 11-JV-11242306-065, and USDA National Institute of Food and Agriculture Hatch project 209145. Any opinions, findings, conclusions, or recommendations expressed in the manuscript are those of authors and do not reflect the views and policies of funding agencies.

LITERATURE CITED

Anandhi A, Zion MS, Gowda PH, Pierson DC, Lounsbury D, Frei A (2013) Past and future changes in frost day indices in Catskill Mountain region of New York. Hydrol Processes 27:3094–3104

Barichivich J, Briffa KR, Osborn TO, Melvin TM, Caesar J (2012) Thermal growing season and timing of biospheric carbon uptake across the Northern Hemisphere. Global

Biogeochem Cycles 26:GB4015
Christiansen DE, Markstrom SL, Hay LE (2011) Impacts of climate change on the growing season in the United States. Earth Interact 15:1–17
Christidis N, Stott PA, Brown S, Karoly DJ, Caesar J (2007) Human contributions to the lengthening of the growing season during 1950–99. J Clim 20:5441–5454
Collins M, Knutti R, Arblaster J, Dufresne JL and others (2013) Long-term climate change: projections, commitments and irreversibility. In: Stocker TF, Qin D, Plattner GK, Tignor M and others (eds) Climate change 2013: the physical science basis. Contribution of Working Group I to the Fifth Assessment Report of the Intergovernmental Panel on Climate Change. Cambridge University Press, Cambridge
Cooter E, LeDuc S (1995) Recent frost date trends in the northeastern United States. Int J Climatol 15:65–75
Cosgrove BA, Lohmann D, Mitchell KE, Houser PR and others (2003) Real-time and retrospective forcing in the North American Land Data Assimilation System (NLDAS) project. J Geophys Res 108:8842
Easterling DR (2002) Recent changes in frost days and the frost-free season in the United States. Bull Am Meteorol Soc 83:1327–1332
Easterling DR, Peterson TC, Gallo KP, Robinson DA, Trenberth KE, Dai A (2000) Observed climate variability and change of relevance to the biosphere. J Geophys Res 105:20101–20114
Feng S, Hu Q (2004) Changes in the agro-meteorological indicators in the contiguous United States: 1951–2000. Theor Appl Climatol 78:247–264
Giorgi F (2006) Regional climate modeling: status and perspectives. J Phys IV 139:101–118
Hayhoe K, Wake CP, Huntington TG, Luo L and others (2007) Past and future changes in climate and hydrological indicators in the US Northeast. Clim Dyn 28:381–407
Jones GV (2005) Climate change in the western United States grape growing regions. Acta Hortic 41–60
Kalnay E, Kanamitsu M, Kistler R, Collins W and others (1996) The NCEP/NCAR 40-year reanalysis project. Bull Am Meteorol Soc 77:437–471
Kanamitsu M, Ebisuzaki W, Woollen J, Yang SK, Hnilo JJ, Fiorino M, Potter GL (2002) NCEP-DOE AMIP-II reanalysis (R-2). Bull Am Meteorol Soc 83:1631–1643
Knutti R, Sedláček J (2013) Robustness and uncertainties in the new CMIP5 climate model projections. Nat Clim Change 3:369–373
Kunkel KE, Easterling DR, Hubbard K, Redmond K (2004) Temporal variations in frost-free season in the United States: 1895–2000. Geophys Res Lett 31:L03201
Kunkel KE, Stevens LE, Stevens SE, Sun L and others (2013a) Regional climate trends and scenarios for the US national climate assessment. 1. Climate of the northeast US NOAA Technical Report NESDIS 142-1, US Department of Commerce, Washington, DC
Kunkel KE, Stevens LE, Stevens SE, Sun L and others (2013b) Regional climate trends and scenarios for the US national climate assessment. 3. Climate of the Midwest US NOAA Technical Report NESDIS 142-3, US Department of Commerce, Washington, DC
Kunkel KE, Stevens LE, Stevens SE, Sun L and others (2013c) Regional climate trends and scenarios for the US national climate assessment. 4. Climate of the US Great Plains. NOAA Technical Report NESDIS 142-4, US Department of Commerce, Washington, DC
Kunkel KE, Stevens LE, Stevens SE, Sun L and others (2013d) Regional climate trends and scenarios for the US national climate assessment. 5. Climate of the southwest US NOAA Technical Report NESDIS 142-5, US Department of Commerce, Washington, DC
Kunkel KE, Stevens LE, Stevens SE, Sun L and others (2013e) Regional climate trends and scenarios for the US national climate assessment. 6. Climate of the northwest US NOAA Technical Report NESDIS 142-6, US Department of Commerce, Washington, DC
Kunkel KE, Stevens LE, Stevens SE, Sun L and others (2013f) Regional climate trends and scenarios for the US national climate assessment. 2. Climate of the southeast US NOAA Technical Report NESDIS 142-2, US Department of Commerce, Washington, DC
Kunkel KE, Stevens LE, Stevens SE, Sun L, Janssen E, Wuebbles D, Dobson JG (2013g) Regional climate trends and scenarios for the US national climate assessment. 9. Climate of the contiguous United States. NOAA Technical Report NESDIS 142-9, US Department of Commerce, Washington, DC
Linderholm H (2006) Growing season changes in the last century. Agric For Meteorol 137:1–14
Luo L, Robock A, Mitchell KE, Houser PR and others (2003) Validation of the North American Land Data Assimilation System (NLDAS) retrospective forcing over the southern Great Plains. J Geophys Res 108:8843
Maloney ED, Camargo SJ, Chang E, Colle B and others (2014) North American climate in CMIP5 experiments. III. Assessment of twenty-first-century projections. J Clim 27:2230–2270
McCabe GJ, Betancourt JL, Feng S (2015) Variability in the start, end, and length of frost-free periods across the conterminous United States during the past century. Int J Climatol 35:4673–4680
Mearns LO, McGinnis S, Arritt R, Biner S and others (2007) The North American Regional Climate Change Assessment Program dataset. National Center for Atmospheric Research Earth System Grid data portal, Boulder, CO. Data downloaded 23 August 2013
Mearns LO, Gutowski W, Jones R, Leung R, McGinnis S, Nunes A, Qian Y (2009) A regional climate change assessment program for North America. EOS Trans AGU 90:311–312
Mearns LO, Arritt R, Biner S, Bukovsky MS and others (2012) The North American Regional Climate Change Assessment Program: overview of phase I results. Bull Am Meteorol Soc 93:1337–1362
Mearns LO, Lettenmaier DP, McGinnis S (2015) Uses of results of regional climate model experiments for impacts and adaptation studies: the example of NARCCAP. Curr Clim Change Rep 1:1–9
Meehl GA, Arblaster JM, Branstator G (2012) Mechanisms contributing to the warming hole and the consequent US east–west differential of heat extremes. J Clim 25: 6394–6408
Melillo JM, Richmond TC, Yohe GW (eds) (2014) Climate change impacts in the United States: the third national climate assessment. US Global Change Research Program, Washington, DC
Menzel A (2003) Plant phonological anomalies in Germany and their relationship to air temperature and NAO. Clim Change 57:243–263
Mote PW, Abatzoglou JT, Kunkel KE (2013) Climate variability and change in the past and the future. In: Dalton

MM, Mote PW, Snover AK (eds) Climate change in the northwest: implications for our landscapes, waters, and communities. Island Press, Washington, DC, p 25–40

Nakičenovič NJ, Alcamo J, Davis G, de Vries B and others (2000) Special report on emissions scenarios: a special report of Working Group III of the Intergovernmental Panel on Climate Change. Cambridge University Press, Cambridge. www.grida.no/climate/ipcc/emission/index.htm

Nemani RR, White MA, Cayan DR, Jones GV, Running SW, Coughlan JC, Peterson DL (2001) Asymmetric warming over coastal California and its impact on the premium wine industry. Clim Res 19:25–34

Pan Z, Arritt RW, Takle ES, Gutowski WJ Jr, Anderson CJ, Segal M (2004) Altered hydrologic feedback in a warming climate introduces a 'warming hole'. Geophys Res Lett 31:L17109

Patricola CM, Cook KH (2013) Mid-twenty-first century warm season climate change in the Central United States. I. Regional and global model predictions. Clim Dyn 40:551–568

Peacock S (2012) Projected twenty-first-century changes in temperature, precipitation, and snow cover over North America in CCSM4. J Clim 25:4405–4429

Pryor SC, Barthelmie RJ, Schoof JT (2013) High-resolution projections of climate-related risks for the Midwestern USA. Clim Res 56:61–79

Romero-Lankao P, Smith JB, Davidson DJ (2014) North America. In: Barros VR, Field CB, Dokken DJ, Mastrandrea MD and others (eds) Climate change 2014: impacts, adaptation, and vulnerability. B. Regional aspects. Contribution of Working Group II to the Fifth Assessment Report of the Intergovernmental Panel on Climate Change. Cambridge University Press, Cambridge, p 1439–1498

Salzmann N, Mearns LO (2012) Assessing the performance of multiple regional climate model simulations for seasonal mountain snow in the Upper Colorado River Basin. J Hydrometeorol 13:539–556

Sheffield J, Barett AP, Colle B (2013) North American climate in CMIP5 experiments. I. Evaluation of historical simulations of continental and regional climatology. J Clim 26:9209–9245

Taylor KE (2001) Summarizing multiple aspects of model performance in a single diagram. J Geophys Res 106: 7183–7192

Taylor KE, Stouffer RJ, Meehl GA (2012) An overview of CMIP5 and the experiment design. Bull Am Meteorol Soc 93:485–498

Tebaldi C, Hayhoe K, Arblaster JM, Meehl GA (2006) Going to the extremes: an intercomparison of model-simulated historical and future changes in extreme events. Clim Change 79:185–211

Thibeault JM, Seth A (2014) Changing climate extremes in the Northeast United States: observations and projections from CMIP5. Clim Change 127:273–287

United States Environmental Protection Agency (USEPA) (2014) Climate change indicators in the United States, 2014, 3rd edn. www.epa.gov/climatechange/indicators/. (accessed 19 February 2016)

Vitasse Y, Lenz A, Körner C (2014) The interaction between freezing tolerance and phenology in temperate deciduous trees. Front Plant Sci 5:541

Walsh J, Wuebbles D, Hayhoe K, Kossin J and others (2014) Our changing climate. Climate change impacts in the United States. In: Melillo JM, Richmond T, Yohe GW (eds) The third national climate assessment. US Global Change Research Program, p 19–67

Weaver CP, Lempert RJ, Brown C, Hall JA, Revell D, Sarewitz D (2013) Improving the contribution of climate model information to decision making: the value and demands of robust decision frameworks. Wiley Interdiscip Rev Clim Change 4:36–60

Wilby RL, Dessai S (2010) Robust adaptation to climate change. Weather 65:180–185

Winkler JA, Guentchev GS, Liszewska M, Perdinan, Tan PN (2011) Climate scenario development and applications for local/regional climate Change impact assessments: an overview for the non-climate scientist. Geogr Compass 5:301–328

Winkler JA, Cinderich AB, Ddumba SD, Doubler D and others (2013a) Understanding the impacts of climate on perennial crops. In: Pielke RA Sr, Niyogi D (eds) Climate vulnerability: understanding and addressing threats to essential resources. 2. Vulnerability of food resources to climate. Elsevier, London, p 37–49

Winkler JA, Andresen JA, Bisanz J, Guentchev GS and others (2013b) Michigan's tart cherry industry: vulnerability to climate variability and change. In: Pryor SC (ed) Climate change in the Midwest: impacts, risks, vulnerability and adaptation. Indiana University Press, Bloomington, IN, p 104–116

Zängl G (2002) An improved method for computing horizontal diffusion in a sigma-coordinate model and its application to simulations over mountainous topography. Mon Weather Rev 130:1423–1432

Zhong S, Chow FK (2013) Meso- and fine-scale modeling over complex terrain: parameterizations and applications. In: Chow FK, DeWekker SFJ, Snyder B (eds) Mountain weather research and forecasting. Springer, Berlin, p 591–653

Editorial responsibility: Eduardo Zorita, Geesthacht, Germany

Submitted: February 25, 2016; Accepted: December 12, 2016
Proofs received from author(s): March 12, 2017